

Selecting Forensic Features for Robust Source Camera Identification

Yongjian Hu^{1,2}, Chang-Tsun Li¹

¹Department of Computer Science,
University of Warwick
Coventry CV4 7AL, UK

e-mail: eeyjhu@scut.edu.cn, c-t.li@warwick.ac.uk

Changhui Zhou³

²School of Electronic and Information Engineering,

³College of Automation Science and Engineering,
South China University of Technology

Guangzhou 510641, China

e-mail: 394306834@qq.com

Abstract—Statistical image features play an important role in forensic identification. Current source camera identification schemes select image features mainly based on classification accuracy and computational efficiency. For forensic investigation purposes, however, these selection criteria are not enough. Consider most real-world photos may have undergone common image processing due to various reasons, source camera classifiers must have the capability to deal with those processed photos. In this work, we first build a sample camera classifier using a combination of popular image features, and then reveal its deficiency. Based on our experiments, suggestions for the design of robust camera classifiers are given.

Keywords—Digital image forensics, camera identification, image feature selection, robust camera classifier, pattern classification

I. INTRODUCTION

Influenced by classical steganalysis (e.g. [1] and [2]), the use of statistical image features becomes common for source imaging device (e.g., camera, scanner) identification. Source imaging device identification can be thought of as a process of steganalysis if device noise in images is regarded as a disturbance caused by externally embedded messages. As a result, the statistics of the images captured by different cameras are believed to be different.

A variety of image features have been proposed and studied in prior arts of steganalysis. In [1], Farid and Lyu found that strong higher-order statistical regularities exist in the wavelet-like decomposition of a natural image, and the embedding of a message significantly alters these statistics and thus becomes detectable. Two sets of image features were studied. The mean, variance, skewness and kurtosis of the subband coefficients form the first feature set while the second feature set is based on the errors in an optimal linear predictor of coefficient magnitude. A total of 216 features were extracted from the wavelet decomposed image to form the feature vector. Support vector machines (SVM) were employed to detect statistical deviations. In [2], Avcibas et al. proved that steganographic schemes leave statistical evidence that can be exploited for detection with the aid of image quality features and multivariate regression analysis. To detect the difference between cover and stego images, 19 image quality metrics (IQMs) were proposed as steganalysis tools.

Statistical image features were introduced for forensic image investigation as soon as this research field emerged. In one early camera identification scheme [3], Kharrazi et al. studied a set of features that designate the characteristics of a specific digital camera to classify test images as originating from a specific camera. CFA (color filter array) configuration, demosaicing algorithms and color processing/transformation were believed to have great impact on the output image of camera. Thus, three average values in RGB channels of an image, three correlations between different color bands, three neighbor distribution centers of mass in RGB channels as well as three energy ratios between different color bands were used for reflecting color features. Moreover, each color band of the image was performed with wavelet decomposition, and the mean of each subband was calculated, just as in [1]. In addition to color features, 13 IQMs were borrowed from [2] to describe the characteristics of image quality. The average identification accuracy for their SVM classifier was 88.02%. This scheme was re-implemented on different camera brands and models in [4].

In one early scanner identification scheme [5], Gou et al. proposed a total of $30+18+12=60$ statistical noise features to reflect the characteristics of the scanner imaging pipeline and motion system. The mean and STD (standard deviation) features were extracted using 4 filters (i.e., averaging filter, Gaussian filter, median filter, and Wiener adaptive filters with 3×3 and 5×5 neighborhood) in each of three color bands to form the first $2\times 5\times 3=30$ features. The STD and goodness of Gaussian fitting were extracted from the wavelet decomposed image of each color band in 3 orientations to form another $2\times 3\times 3=18$ wavelet features. Two neighborhood prediction errors were calculated from each color band at two brightness levels to form the last $2\times 3\times 2=12$ features. The outcome of their SVM classifier had an identification accuracy over 95%.

Another scanner identification scheme was proposed by Khanna et al. [6]. Unlike [5] that used three types of features, only statistical properties of the sensor pattern noise (SPN) were used. The SPN was first proposed for correlation-based camera identification in [7]. The major component of SPN is the photo response non-uniformity noise (PRNU). Due to the similarity between camera and scanner pipelines, the PRNU-based detection was extended for scanner identification. However, the camera fingerprint is a 2-D spread-spectrum

signal while the scanner fingerprint is a 1-D signal. So Khanna et al. proposed a special way to calculate the statistical features of the linear PRNU. The mean, STD, skewness, and kurtosis of the row correlations and the column correlations form the first eight features on each color channel of the input image. The STD, skewness, and kurtosis of the average of all rows and the average of all columns form the next six features. The last feature for every color channel is representative of the relative difference in periodicity along the row and column directions of the sensor noise. The results from their SVM-based classifier were often better than those in [5]. The robustness of this PRNU features-based scanner classifier was evaluated when subject to JPEG compression, contrast stretching and sharpening.

Other image features-based schemes include [8]-[10]. In [8], four sets of image features related to PRNU were used. In [9], the impact of image content on camera identification rates was analyzed. In [10], several feature selection schemes were implemented with SVM-based classifiers. The optimal subset of features was defined as the one which has the highest identification precision rate, and meanwhile has redundant or irrelevant features removed.

There are many statistical image features available for camera identification. It seems not difficult to select some commonly used features to generate a pattern classification-based camera identifier with good detection rates. In this work, we first give an example to build such a classifier, and then reveal its deficiency. Based on our experiments, we discuss the issues about the design of a practical camera classifier. Our work is initially motivated by [14], where the reliability of forensic techniques was discussed.

II. A SAMPLE CAMERA CLASSIFIER

A. Construction of Feature Vector

For simplicity of description, we call wavelet features, color features, IQMs, statistical features of difference images, and statistical features of prediction errors Feature Sets I, II, III, IV, and V, respectively. These features are popular ones in literature. We select them to form a new feature vector for our sample classifier. Below we explain how to calculate them.

Feature Set I describes the correlation between the subband coefficients. We choose the mean, variance, skewness and kurtosis of high-frequency subband coefficients at each orientation and at scales. Using biorthogonal 9/7 wavelet filters, we perform one-scale wavelet transform on each color band. $3 \times 3 \times 4 = 36$ features are acquired.

Feature Sets II and III are obtained in a way similar to [3] and [4]. Feature Set II consists of $3+3+3+3=12$ color features including the average value of each color band, the correlation pair between two different color bands, the neighbor distribution center of mass for each color band and three energy ratios, namely $E1 = |G|^2 / |B|^2$, $E2 = |G|^2 / |R|^2$, and $E3 = |B|^2 / |R|^2$. Feature Set III consists of $3+3+6=12$ IQMs including three pixel difference-based features, i.e.,

Minkowski difference (1), mean absolute error (2) with $\gamma=1$, and mean square error (2) with $\gamma=2$; three correlation-based features, i.e., structural content (3), normalized cross correlation (4), and Czekonowski correlation (5); six spectral features, i.e., spectral magnitude error (6), spectral phase error (7), spectral phase-magnitude error (8), block spectral magnitude error (9), block spectral phase error (10), and block spectral phase-magnitude error (11).

$$\varepsilon^\infty = \max_{i,j} \sum_{k=1}^K \frac{1}{K} \left| C_k(i,j) - \tilde{C}_k(i,j) \right| \quad (1)$$

$$M1 = \frac{1}{K} \sum_{k=1}^K \left\{ \frac{1}{N^2} \sum_{i,j=1}^N \left| C_k(i,j) - \tilde{C}_k(i,j) \right|^\gamma \right\}^{1/\gamma} \quad (2)$$

$$C1 = \frac{1}{K} \sum_{k=1}^K \frac{\sum_{i,j=1}^N C_k^2(i,j)}{\sum_{i,j=1}^N \tilde{C}_k^2(i,j)} \quad (3)$$

$$C2 = \frac{1}{K} \sum_{k=1}^K \frac{\sum_{i,j=1}^N C_k(i,j) \tilde{C}_k(i,j)}{\sum_{i,j=1}^N C_k^2(i,j)} \quad (4)$$

$$C3 = \frac{1}{N^2} \sum_{i,j=1}^N \left\{ 1 - \frac{2 \sum_{k=1}^K \min(C_k(i,j), \tilde{C}_k(i,j))}{\sum_{k=1}^K (C_k(i,j) + \tilde{C}_k(i,j))} \right\} \quad (5)$$

$$S = \frac{1}{N^2} \sum_{u,v=1}^N \left| M(u,v) - \tilde{M}(u,v) \right|^2 \quad (6)$$

$$S1 = \frac{1}{N^2} \sum_{u,v=1}^N \left| \varphi(u,v) - \tilde{\varphi}(u,v) \right|^2 \quad (7)$$

$$S2 = \frac{1}{N^2} (\lambda \sum_{u,v=1}^N \left| \varphi(u,v) - \tilde{\varphi}(u,v) \right|^2 + \quad (8)$$

$$(1-\lambda) \sum_{u,v=1}^N \left| M(u,v) - \tilde{M}(u,v) \right|^2$$

$$S3 = \text{median}_l J_M^l \quad (9)$$

$$S4 = \text{median}_l J_\phi^l \quad (10)$$

$$S5 = \text{median}_l J^l \quad (11)$$

where C and \tilde{C} represent the original image and its denoised version, respectively. (i,j) and (u,v) are the coordinates of an image pixel in spatial and transform domains, respectively. $N \times N$ is the image size. $K (= 3)$ refers to three color bands. $\gamma = 1, 2$, $\Gamma_k(u,v)$ is the DFT of the k^{th} band image. $M(u,v) = |\Gamma(u,v)|$, $\varphi(u,v) = \arctan(\Gamma(u,v))$, $\lambda = 2.5 \times 10^{-5}$,

$$J_M^l = \frac{1}{K} \sum_{k=1}^K \left\{ \sum_{u,v=1}^N \left(|\Gamma_k^l(u,v)| - |\tilde{\Gamma}_k^l(u,v)| \right)^\gamma \right\}^{1/\gamma},$$

$$J_\phi^l = \frac{1}{K} \sum_{k=1}^K \left\{ \sum_{u,v=1}^b \left(|\phi_k^l(u,v)| - |\tilde{\phi}_k^l(u,v)| \right)^\gamma \right\}^{1/\gamma}, \quad J^l = \lambda J_M^l + (1-\lambda) J_\phi^l,$$

l is the number of blocks. b is the block size. Empirically, $b=32$. The reader is referred to [11] for more detailed information about (1)-(11).

In order to obtain Feature Set IV, the averaging filter, Gaussian filter, median filter, and Wiener adaptive filters with 3×3 and 5×5 neighborhood are separately used to acquire the difference images. Similar to [5], we first perform the absolute operation on the difference images, and then take \log_2 transformation. Afterwards, we calculate the mean and STD of the \log_2 -transformed absolute values. $2 \times 5 \times 3 = 30$ features are obtained.

Feature Set V consists of $2 \times 2 \times 3 = 12$ statistical features of prediction errors. Strong correlation exists across a natural image, in particular, in smooth regions. Thus, pixel values in smooth regions can be predicted from their neighboring pixels with high accuracy. For images from different cameras, however, linear prediction error is probably different. The mean and STD of linear prediction errors are then used as statistical features of prediction errors. The way in [5] is borrowed to obtain Feature Set V.

B. Experiments

The above five feature sets form our feature vector of $36+12+12+30+12=102$ dimensions. We use this vector as the input of a camera classifier. Since the LIBSVM toolbox [12] with a nonlinear RBF kernel is frequently used for camera/scanner identification in literature, we adopt it in our experiments for the sake of comparison.

Ten cameras are used. They are five Canon cameras: A40, A620-1, A620-2, A720, 450D; two Nikon cameras: L3-1, L3-2; two Sony cameras: DSC-T10, DSC-W90; one Olympus camera: U820. For simplicity, we index the above ten cameras as X1, X2, X3, X4, X5, X6, X7, X8, X9, and X10, respectively. To evaluate the capability of these image features in identifying specific cameras, we use two Canon A620 cameras, i.e., A620-1 and A620-2, and two Nikon L3 cameras, i.e., L3-1 and L3-2. The photos taken by Canon A620-2 (i.e., X3) and Nikon L3-2 (i.e., X7) are downloaded from <http://www.flickr.com/>. Each camera takes 300 photos of natural scenes including buildings, trees, blue sky and clouds, streets and people. All the photos are saved in JPEG format at the highest resolution each camera can support. For a fair comparison, we take a 1024×1024 test image block from each photo. Based on our previous analysis [13], each test image is cropped from the center of a photo to avoid saturated image regions. This selection strategy makes the test image better reflect the original image content. For each camera, we randomly choose 150 images to form the training set; the rest 150 images form the test set. Experimental results are shown in the form of confusion matrix, where the first column and the first row are the test camera index and the predicted camera index, respectively. For clarity of

comparison, the classification rate below 3% is simply denoted as *.

From Table 1, our classifier achieves the average accuracy of at least 95% for all cameras except X3 and X7. This result proves that our feature vector is very effective. As for X3 and X7, the correct rates are 88% and 62%, respectively. We owe the decline in accuracy to different image content. The photos taken by X3 and X7 are downloaded from the internet. It can not be confirmed whether the photos have been altered. The only thing we can observe is that the former image set consists of artificial products with various textile patterns and the image content is usually bright while the latter image set mainly consists of indoors scenes and the image content is usually dark. In contrast, our photos are mainly natural scenes with middle intensity. Our detection results coincide with the observation that identification rate is affected by image content [9, 13].

Using Tables 2-6, we further investigate the performance of each individual feature set. According to Table 2, the wavelet features have almost the same identification power as the five feature sets all put together. From Table 5, the statistical features of difference images also have good performance. Such results are reasonable because these two feature sets are based on the high-frequency component of an image. On the other hand, the IQMs and statistical features of prediction errors only have moderate performance according to the results in Tables 4 and 6. In particular, the color features only lead to the accuracy of 47%, as shown in Table 3. It seems that this feature set contributes the least to our sample classifier.

III. ROBUSTNESS OF OUR SAMPLE CLASSIFIER

For real-world applications, camera identifiers should have the capability in tackling images that have undergone different image manipulations. Some manipulations are probably not malicious attacks but normal ways for saving storage space or emphasizing part of image content. We evaluate the robustness of our classifier under three common image manipulations: JPEG compression, cropping, and scaling. Note that each test image has undergone only one type of manipulation for each case. We do not consider the combined effect of different manipulations to avoid making the analysis too complex.

A. Experimental Results under Compression

We take JPEG compression with quality factor 70. From Table 7, the average accuracy is 43%. Compared with Table 1, the performance of the classifier greatly decreases. We further investigate the performance of each individual feature set. From Feature Sets I to V, the correct identification rates are 21%, 46%, 31%, 24%, and 33%, respectively. Apparently, the performance of each feature set degrades. Among them, Feature Set I has the sharpest decline in performance (see Table 8). The possible reason is that compression makes more high-frequency coefficients equal zero. On the other side, the performance of Feature Set II is a little surprising. The classifier has the average accuracy of 46%. Compared with the accuracy before compression (47%), there is only a slight decline. This implies that

compression has little impact on Feature Set II (color features).

B. Experimental Results under Cropping

We remove 1/8 image region from the original image to simulate a cropping manipulation. According to Table 9, the average accuracy is 39%. From Feature Sets I to V, the correct identification rates are 35%, 32%, 25%, 84%, and 25%, respectively. It can be seen that Feature Sets III and V are more sensitive to cropping. The possible reason is that the pixels in the removed image regions are replaced with value 0 and such replacement affects the measurement of IQMs (see Table 10). Meanwhile, the removed and replaced regions can be thought of as smooth regions. Their appearance probably affects the performance of statistical features of prediction errors (see Table 11). In contrast, Feature Set IV maintains good performance. Thus, cropping does not affect Feature Set IV (statistical features of difference images) too much.

C. Experimental Results under Scaling

We shrink the test images with scaling factor 0.9. According to Table 12, the accuracy is 53%. From Feature Sets I to V, the correct identification rates are 32%, 47%, 39%, 58%, and 49%, respectively. Feature Set I has the greatest decline in performance (see Table 13). The possible reason is that wavelet features are fragile to geometrical distortions such as scaling. On the other side, Feature Set IV (statistical features of difference images) still has the best performance. In other words, Feature Set IV is not very sensitive to small scaling operations.

IV. CONCLUSIONS

The issue of selecting image features for robust camera identification has not been thoroughly addressed in literature. In this paper, we have shown (i) some features (e.g., wavelet features) may perform well for intact images, but are sensitive to image processing; other features (e.g., color features) may have mediocre performance for intact images, but have some robustness to image processing; (ii) different image manipulations have different effects on image features.

The problem of camera identification is a complex one with no universally applicable solution. Our efforts in this work only reveal the deficiency of a camera classifier which has been designed without considering the robustness against common image processing. It is inferred from our experiments that the use of many different types of image features can benefit the robustness of camera classifiers. Moreover, even when decreasing the number of features for the sake of computational efficiency, the selection of reduced feature set has to take the robustness into account. The selection of suitable feature set is our future work.

ACKNOWLEDGMENT

This work was supported by NSF of China 60772115.

REFERENCES

- [1] H. Farid and S. Lyu, "Detecting hidden messages using higher-order statistics and support vector machines," Proc. of 5th Int. Workshop on Information Hiding, Springer-Verlag, Berlin, Heidelberg, vol. 2578, pp. 340-354, 2002.
- [2] I. Avciabas, N. Memon, B. Sankur, "Steganalysis using image quality metrics," IEEE Trans. on Image Process., vol. 12, no. 2, pp. 221-229, Jan. 2003.
- [3] M. Kharrazi, H.T. Sencar, and N. Memon, "Blind source camera identification," Proc. of IEEE Int. Conf. on Image Processing, Singapore, pp. 709-712, Oct. 24-27, 2004.
- [4] M.-J. Tsai and G.-H. Wu, "Using image features to identify camera sources," Proc. of IEEE Int. Conf. on Acoustics, Speech and Signal Processing, vol. 2, 2006.
- [5] H. Gou, A. Swaminathan, and M. Wu, "Intrinsic sensor noise features for forensic analysis on scanners and scanned images," IEEE Trans. on Inf. Forensics Security, vol. 4, no. 3, pp. 476-491, Sept. 2009.
- [6] N. Khanna, A.K. Mikkilineni, and E.J. Delp, "Scanner identification using feature-based processing and analysis," IEEE Trans. on Inf. Forensics Security, vol. 4, no. 1, pp. 123-139, Mar. 2009.
- [7] J. Lukas, J. Fridrich, and M. Goljan, "Digital camera identification from sensor pattern noise," IEEE Trans. on Inf. Forensics Security, vol. 1, no. 2, pp. 205-214, Jun. 2006.
- [8] T. Filler, J. Fridrich, and M. Goljan, "Using sensor pattern noise for camera model identification," Proc. of IEEE Int. Conf. on Image Processing, pp. 1296-1299, 2008.
- [9] M.-J. Tsai, C.-L. Lai, and J. Liu, "Camera/Mobile phone source identification for digital forensics," Proc. of IEEE Int. Conf. on Acoustics, Speech and Signal Processing, pp. 221-224, 2007.
- [10] M.-J. Tsai and C.-S. Wang, "Adaptive feature selection for digital camera source identification," Proc. of IEEE Int. Symposium on Circuits and Systems, May 2008.
- [11] I. Avciabas. Image quality statistics and their use in steganalysis and compression. Ph.D. Thesis, Bogazici University 2001.
- [12] C.-C. Chang and C.-J. Lin, LIBSVM: A Library for Support Vector Machines 2001. <http://www.csie.ntu.edu.tw/~cjlin/>
- [13] C.-T. Li, "Source camera identification using enhanced sensor pattern noise," IEEE Trans. on Inf. Forensics Security, vol. 5, no. 2, pp. 280-287, Jun. 2010.
- [14] T. Gloe, M. Kirchner, P. Winkler, and R. Bohme, "Can we trust digital image forensics," Proc. of the 15th International Conference on Multimedia, Sept. 2007.

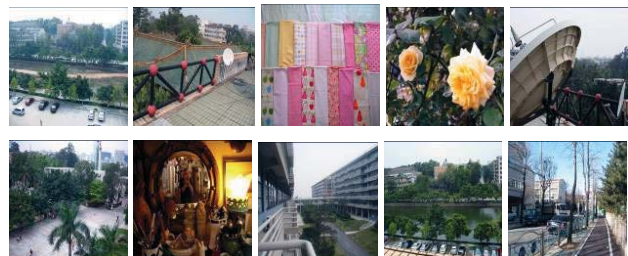


Figure 1. Test photos, from left to right, top to bottom, taken by cameras X1, X2, X3, X4, X5, X6, X7, X8, X9, and X10.

Table 1. Confusion matrix for our sample classifier using all the five feature sets. Accuracy = 92% (1383/1500)

	X1	X2	X3	X4	X5	X6	X7	X8	X9	X10
X1	97	*	*	*	*	*	*	*	*	*
X2	3	95	*	*	*	*	*	*	*	*
X3	*	*	88	6	*	*	*	*	*	*
X4	*	*	*	96	*	*	*	*	*	*
X5	*	*	*	*	98	*	*	*	*	*
X6	*	*	*	*	*	98	*	*	*	*
X7	*	*	*	*	21	8	61	*	*	5
X8	*	*	*	*	*	*	*	99	*	*
X9	*	*	*	*	*	*	*	*	95	*
X10	*	*	*	*	*	*	*	*	*	95

Table 5. Confusion matrix for our sample classifier using only Feature Set IV. Accuracy = 85% (1277/1500)

	X1	X2	X3	X4	X5	X6	X7	X8	X9	X10
X1	83	10	*	*	*	*	*	*	*	*
X2	12	85	*	*	*	3	*	*	*	*
X3	*	*	87	7	*	*	*	*	*	*
X4	*	*	*	87	*	*	*	*	5	*
X5	*	*	*	*	99	*	*	*	*	*
X6	5	*	*	*	*	83	4	*	3	*
X7	*	*	*	*	10	*	73	*	7	3
X8	*	*	*	*	*	*	*	95	*	*
X9	5	*	*	*	*	*	4	8	75	*
X10	4	*	*	*	5	*	3	*	*	85

Table 2. Confusion matrix for our sample classifier using only Feature Set I. Accuracy = 92% (1382/1500)

	X1	X2	X3	X4	X5	X6	X7	X8	X9	X10
X1	95	*	*	*	*	*	*	*	*	*
X2	*	97	*	*	*	*	*	*	*	*
X3	*	*	83	7	*	*	7	*	*	*
X4	*	*	*	91	*	6	*	*	*	*
X5	*	*	*	*	94	*	*	*	*	*
X6	*	*	*	*	*	95	*	*	*	*
X7	*	*	*	*	5	3	87	*	*	*
X8	*	3	*	*	*	*	*	97	*	*
X9	5	*	*	*	*	*	*	*	91	*
X10	*	*	*	*	*	*	6	*	*	93

Table 6. Confusion matrix for our sample classifier using only Feature Set V. Accuracy = 59% (898/1500)

	X1	X2	X3	X4	X5	X6	X7	X8	X9	X10
X1	83	3	*	*	*	5	*	*	*	*
X2	10	43	*	5	5	23	*	*	6	3
X3	*	5	73	7	*	*	*	5	*	4
X4	*	4	7	67	*	7	*	5	*	3
X5	*	*	*	*	85	*	*	5	*	5
X6	*	21	4	5	*	53	*	*	10	*
X7	3	5	3	5	9	*	45	8	12	7
X8	*	*	*	*	26	*	*	59	*	4
X9	*	7	5	5	11	9	*	10	40	8
X10	5	*	*	5	16	4	*	11	*	52

Table 3. Confusion matrix for our sample classifier using only Feature Set II. Accuracy = 47% (702/1500)

	X1	X2	X3	X4	X5	X6	X7	X8	X9	X10
X1	64	*	*	*	6	8	*	*	9	7
X2	20	40	*	*	13	9	*	3	8	5
X3	*	*	81	3	*	7	*	*	*	3
X4	7	17	*	45	4	9	*	5	*	9
X5	4	7	*	5	38	17	*	3	12	9
X6	15	6	*	12	11	43	*	3	6	*
X7	6	9	13	7	7	*	43	*	9	4
X8	3	11	*	7	24	15	*	29	*	5
X9	9	10	7	9	13	13	*	3	35	*
X10	*	5	*	9	4	12	*	10	5	51

Table 7. Confusion matrix for our sample classifier using all the five feature sets. Accuracy = 43% (638/1500)

	X1	X2	X3	X4	X5	X6	X7	X8	X9	X10
X1	57	*	5	4	3	15	11	*	*	4
X2	31	21	*	4	4	18	15	*	*	5
X3	17	*	39	*	3	12	21	*	*	5
X4	7	*	*	21	5	7	44	*	*	15
X5	*	*	4	*	73	*	23	*	*	*
X6	4	*	*	*	5	65	21	*	*	*
X7	7	*	*	*	8	5	73	*	*	4
X8	4	3	6	*	19	*	65	*	*	*
X9	13	*	*	*	21	22	35	*	*	*
X10	*	*	*	*	8	*	11	*	*	75

Table 4. Confusion matrix for our sample classifier using only Feature Set III. Accuracy = 66% (987/1500)

	X1	X2	X3	X4	X5	X6	X7	X8	X9	X10
X1	77	7	*	11	*	*	*	*	*	*
X2	20	61	*	9	*	*	*	*	*	*
X3	*	*	81	11	*	*	*	*	*	*
X4	11	13	6	58	*	5	*	*	*	*
X5	5	*	*	*	88	*	5	*	*	*
X6	4	5	*	*	4	70	*	4	10	*
X7	*	7	*	7	12	*	52	5	4	7
X8	*	4	4	5	5	*	17	56	3	*
X9	*	4	*	*	6	11	17	13	45	*
X10	*	*	*	4	3	*	11	9	*	69

Table 8. Confusion matrix for our sample classifier using only Feature Set I. Accuracy = 21% (319/1500)

	X1	X2	X3	X4	X5	X6	X7	X8	X9	X10
X1	12	3	*	*	*	*	79	*	*	4
X2	*	19	*	*	*	*	73	*	*	4
X3	*	*	23	*	*	10	58	*	*	6
X4	*	*	*	12	*	*	74	*	*	10
X5	*	*	*	*	4	*	96	*	*	*
X6	*	*	*	*	*	*	93	*	*	*
X7	*	*	*	*	4	4	87	*	*	*
X8	4	8	*	*	*	*	86	*	*	*
X9	6	*	*	*	12	13	65	*	*	*
X10	*	*	*	*	*	*	46	*	*	53

Table 9. Confusion matrix for our sample classifier using all the five feature sets. Accuracy = 39% (581/1500)

	X1	X2	X3	X4	X5	X6	X7	X8	X9	X10
X1	63	5	7	*	*	*	*	*	*	24
X2	5	57	9	4	*	*	*	*	*	23
X3	*	*	37	57	*	*	*	*	*	5
X4	*	*	7	74	*	*	*	*	*	15
X5	*	*	84	*	*	*	*	*	*	13
X6	*	*	7	13	*	45	*	*	*	31
X7	*	*	65	4	*	*	4	*	*	24
X8	*	11	45	13	*	*	*	6	*	23
X9	3	*	16	5	4	*	*	*	33	37
X10	*	*	30	*	*	*	*	*	*	66

Table 12. Confusion matrix for our sample classifier using all the five feature sets. Accuracy = 53% (793/1500)

	X1	X2	X3	X4	X5	X6	X7	X8	X9	X10
X1	48	*	*	*	*	45	*	*	*	*
X2	24	30	*	*	7	38	*	*	*	*
X3	*	8	71	9	*	*	*	*	*	4
X4	*	20	*	37	11	15	6	*	*	8
X5	3	*	*	*	96	*	*	*	*	*
X6	*	*	*	*	5	89	*	*	*	*
X7	*	*	*	*	20	6	64	*	*	4
X8	5	55	*	*	30	*	7	*	*	*
X9	6	17	*	*	24	30	19	*	*	*
X10	*	*	*	*	3	*	3	*	*	91

Table 10. Confusion matrix for our sample classifier using only Feature Set III. Accuracy = 25% (380/1500)

	X1	X2	X3	X4	X5	X6	X7	X8	X9	X10
X1	49	*	6	23	*	4	3	*	11	*
X2	46	*	7	19	4	11	*	*	9	*
X3	40	*	31	17	*	4	*	*	*	*
X4	31	*	*	24	5	9	*	*	20	*
X5	*	*	8	6	51	*	23	*	*	7
X6	17	*	4	18	10	21	*	*	26	*
X7	3	*	9	21	18	9	25	*	*	9
X8	5	*	5	17	11	17	19	*	19	3
X9	11	*	*	20	25	7	9	*	17	7
X10	9	*	5	14	8	3	13	*	13	31

Table 13. Confusion matrix for our sample classifier using only Feature Set I. Accuracy = 32% (486/1500)

	X1	X2	X3	X4	X5	X6	X7	X8	X9	X10
X1	*	*	*	5	*	70	20	*	*	*
X2	3	3	*	12	*	62	12	*	*	5
X3	*	*	7	57	7	13	13	*	*	*
X4	*	*	*	22	17	37	8	*	*	15
X5	*	9	*	*	77	*	13	*	*	*
X6	*	*	*	*	*	70	23	*	*	*
X7	*	*	*	*	20	*	77	*	*	*
X8	*	11	*	*	39	5	43	*	*	*
X9	*	5	*	*	11	15	63	*	*	*
X10	*	*	*	*	5	*	26	*	*	67

Table 11. Confusion matrix for our sample scheme using Feature Set V. Accuracy = 25% (371/1500)

	X1	X2	X3	X4	X5	X6	X7	X8	X9	X10
X1	90	*	*	*	*	*	4	*	*	*
X2	87	*	*	*	*	*	6	*	*	*
X3	71	9	11	*	*	3	*	*	*	*
X4	61	13	*	5	*	10	5	*	*	4
X5	23	*	*	*	59	*	10	*	4	*
X6	87	*	*	*	*	7	*	*	*	*
X7	27	*	*	*	5	*	50	*	11	*
X8	41	6	*	*	28	*	17	*	*	3
X9	62	6	*	*	*	7	11	*	3	9
X10	39	*	*	*	8	13	12	*	5	21